RELATIONSHIP BETWEEN TASK-BASED MODULATION TRANSFER FUNCTION AND EVALUATION INDEX OF TUMOR AREA IN DUAL ENERGY SUBTRACTION CHEST RADIOGRAPHY

Shu Onodera [1 2 a], *Yongbum Lee* [2], *Tomoyoshi Kawabata* [1],
[1] Department of Radiology, Division of Medical Technology, Tohoku University Hospital, Sendai, Japan,
onodera@rad.hosp.tohoku.ac.jp tomoyoshi.kawabata.c2@tohoku.ac.jp
[2] Graduate School of Health Sciences, Niigata University, Niigata, Japan, lee@clg.niigata-u.ac.jp
[a] Corresponding Author

Abstract – When extracting lesions in medical images using deep learning, the extraction accuracy will be higher if the image quality is good. The purpose of this study is to investigate and comprehend the relationship between the spatial-resolution property of X-ray images and the accuracy of lesion extraction by deep learning, and to examine the possibility of dose reduction from the obtained results. The simulated masses arranged on different areas in dual energy subtraction (DES) chest radiographs acquired by various doses were used for the investigation. Task-based transfer functions (TTFs) as a spatial-resolution property for the DES chest radiography were calculated. The mass areas were also extracted by U-net, and Dice coefficients were obtained as the extraction accuracy. In results, regardless of mass locations, the TTFs of the reference dose images and the 75% dose images showed high frequency responses, and the Dice coefficients were also high. The TTFs and the Dice coefficients were obviously lower in the images of when the masses were located in the right supraclavicular region at 50% dose compared with the other conditions. The results of this study suggested that the spatial-resolution property was strongly related to the accuracy of mass region extracted by deep learning in DES chest radiography. In conclusion, the dose reduction of about 25% compared with the conventional dose should be feasible.

Keywords: deep learning, spatial-resolution property, Dice coefficient, 1-shot dual energy subtraction

1. INTRODUCTION

When the lesion overlaps the bony region in a chest radiograph, the recognition of the lesion will be difficult [1]. As a countermeasure to this problem, an image processing method has been used to subtract the two images obtained by using 2-shots with different tube voltages during one examination. Using this technique, it is possible to obtain an image of soft tissue only (hereafter referred to as soft tissue image) in which the bone shadow is removed by subtracting two types of images with different imaging conditions [1-3]. However, on the 2-shots imaging, acquisition of good subtraction images is sometimes difficult due to poor breath-holding and heartbeat effects caused by extended imaging time. In recent years, there has been a shift from computed radiography (CR) systems to flat panel detector (FPD) imaging [4], and dual energy subtraction (DES) techniques with 1-shot imaging using FPDs stacked with two types of X-ray detectors have become popular. 1-shot imaging has several advantages, such as lower radiation exposure, compared to 2-shots imaging.

The recognition of the lesion will be commonly easy by using DES, because bone shadows are removed in soft tissue images. However, the image quality of chest radiograph differs substantially from region to region due to differences in detector dose and scattered radiation dose, and thus differences in lesion detectability are expected to occur depending on the location of the lesion. In particular, the upper lobe, which is a predilection site of adenocarcinoma [5], is considered to be significantly affected by scattered radiations generated from the clavicle and scapula.

Furthermore, the spatial-resolution property of the imaging system is very important in detecting masses [6]. In general, various image processing has been applied to chest radiograph to improve image quality. Typical examples include multi-frequency processing and dynamic range compression processing. The effects of these processes show nonlinear behavior that is influenced by the image quality of different parts of the image. The image quality of soft tissue images is also expected to exhibit nonlinear behavior, and therefore, task-based evaluation is necessary to determine the spatial-resolution property of soft tissue images.

In addition, as the volume of medical image data increases, computer-aided diagnosis (CAD) systems are being introduced into clinical workflows, and in recent years, deep learning technology has been incorporated into these systems. Image segmentation is the process of dividing the image into regions for each target in the image, or cutting out the target region and distinguishing it from other regions. The target regions in medical images are usually organs and lesions, and not only the features of the objects but also the information of overall location must be identified in the original input image in the segmentation process. In general, the higher quality of the input image is, the higher extraction accuracy is. U-net [7] is a typical deep convolutional neural network for image segmentation. In this study, we focused on the extraction of lung masses using U-net in soft tissue images. We also investigated the relationship between the

evaluation index of the mass region, which indicated the extraction accuracy, and the spatial-resolution property of the soft tissue images. Although there are several reports on lesion detection using visual evaluation in 1-shot DES systems with CR systems [8-12], there are no reports on relationship between the spatial-resolution property of the image and the accuracy of lesion extraction using deep learning in FPD systems. The purpose of this study is to investigate and comprehend the spatial-resolution property of soft tissue images under different doses and locations of masses, and to examine the possibility of dose reduction in DES chest radiography by the investigated relationship.

2. MATERIALS AND METHODS

Acrylic cylinders (20 mm in diameter and 3 mm in thickness) simulating a mass were placed in four regions (right supraclavicular, left middle lung, right lower lung, and mediastinum) on the chest phantom (Fig. 1), and after imaging at different doses (115 kV, 1.6 mAs: reference dose, 1.25 mAs: 75% dose, 0.8 mAs: 50% dose), we acquired soft tissue images processed by DES.

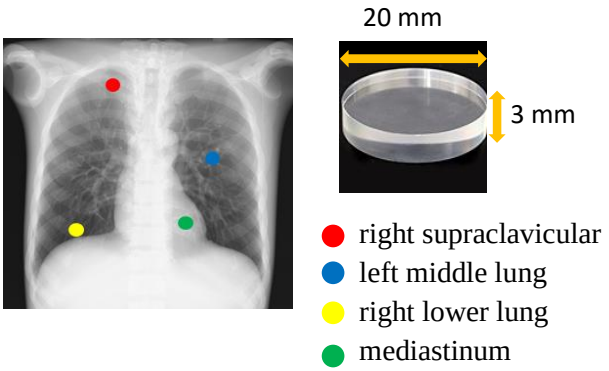

Fig.1 Placement of simulated masses on chest phantom

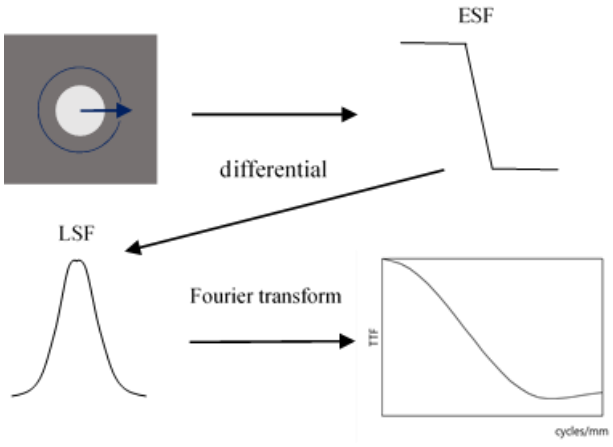

Fig.2 TTF calculation process

The boundary lines of masses in the soft tissue images were manually determined and used to calculate the TTFs [13] as the spatial-resolution property. The process of calculating TTF is shown in Fig. 2. The edge spread function (ESF) of a cylinder was obtained by averaging the profiles across the edges of the cylinder in the radial direction from the center. Next, the TTF was calculated by Fourier transform from the line spread function (LSF), which is the derivative of the LSF. Then, regions of interests (ROIs) including the masses were cropped and resized into 128×128 matrices, and converted to png format. U-net was used for extraction of the mass area from the cropped image. The operating environment of U-net for this study was the following: Windows10, Python3.7, TensorFlow1.13.1, keras2.3.1, Core i7 Intel CPU, 16GByte memory, GeForce GTX 1650 GPU. ReLu and sigmoid functions were used as activation functions. Cross entropy was used as the loss function, and Adam was used as the learning optimization algorithm. In this study, we used the reference dose images as training data and respective dose reduction images as evaluation data. The teaching images were created by binarization of the mass and background regions. The Dice coefficient [14] was obtained to show the degree of similarity between the output images and the teaching images, and was used to evaluate the accuracy of segmentation for the mass region by U-net. Below is the definitional identity of the Dice coefficient.

$$Dice(A,B) = \frac{2|A \cap B|}{|A| + |B|}$$

Here, A is the mass region in the training images and B is the mass region in the segmentation images. Finally, we clarified the relationship between the evaluation index of the mass region and the spatial-resolution property of the soft tissue images from the trend of the values of TTFs and Dice coefficients.

3. RESULTS AND DISCUSSION

Fig. 3 shows the TTFs for each of the conditions. In the apex of the lung, the contrast was low compared with other regions due to scattered radiation from the clavicle and scapula. There was no difference in TTFs between the reference dose images and the 75% dose images, and the TTF of the 50% dose images was lowest. On the other hand, the difference in TTFs among the three doses was small in the middle and lower lung regions, because the effect of scattered radiation was small and the contrast was high. In the mediastinal region, we supposed the TTFs behaved similarly to the apex region due to the low contrast caused by scattered radiation generated from the heart and sternum. However, the TTFs was not as low as in the apex region. The TTFs of the apex region were comprehensively lower than the other regions. The Dice coefficients for the 75% dose images were generally high regardless of the location of the mass or the radiation dose, and their behaviors corresponded with those of the TTFs. In contrast, the Dice

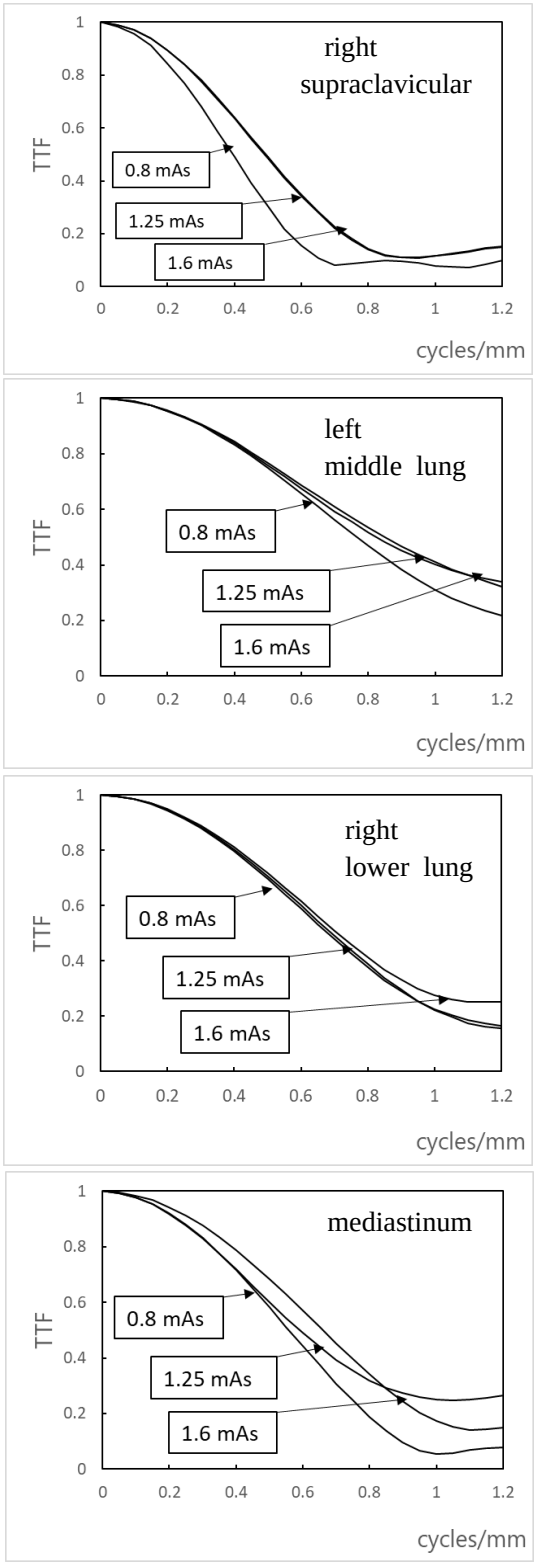

Fig.3 TTFs for each of the conditions

Table.1 Dice coefficients for each of the conditions

mAs	right supraclavicular	left middle lung	right lower lung	mediastinum
1.25	0.960	0.960	0.959	0.971
0.8	0.937	0.969	0.963	0.967

coefficient for the right supraclavicular region under the 50% dose condition was low. It was also consistent with the trend of the TTF (Table 1).

In the 50% dose condition with the simulated mass located on the right clavicle, the TTF was significantly lower and the Dice coefficient was also lower than in the other conditions. Fig. 4 shows the region of the mass extracted by U-net under the 75% and 50% dose conditions. Compared with the 75% dose condition, a slightly larger region against the teaching data was extracted in the 50% dose condition. This phenomenon could happen if the TTF was reduced caused by scattered radiation from the clavicle and scapula, and the increasing of image noise caused by the low dose delivered to the detectors prevented the correct extraction of the mass area. In the mediastinum region, the influence of scattered radiation and detector dose was considered to be large as in the right supraclavicular region. However, the TTF values were not so different from those in the left middle lung field and right lower lung field, and the Dice coefficients were also similar. This may be due to the fact that the area around the mass in the mediastinum region has fewer pulmonary blood vessels and a simpler structure against the other regions. Thus, we considered that the mass area could be extracted with high accuracy despite the large influence of image noise.

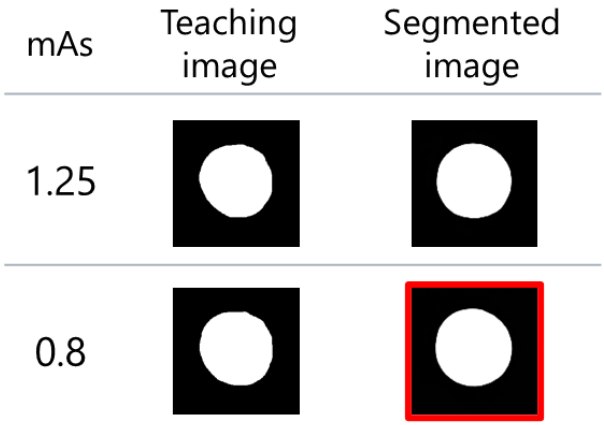

Fig.4 Binary images of masses located on the right supraclavicular region

The results of this study showed that the spatial-resolution properties of soft tissue images were strongly related to the evaluation indexes of extracted mass area by deep learning in reference dose images and 75% dose images. In addition, the spatial-resolution property deteriorated and the evaluation index of the mass region showed low values when the mass originated in the right supraclavicular region under the 50% dose condition. For the above reason, the possibility of dose reduction of about 25% in 1-shot DES chest radiography was suggested. Furthermore, if we could select more suitable parameters of an image processing improving spatial resolution such as multi-frequency processing, further dose reduction would be feasible.

The first limitation of this study is about the shape of the simulated mass. The simulated mass used in this study was a

simple cylindrical structure only. The results might be different if we used masses with more complex structures such as spicules. As the second limitation, the masses were placed in specific four locations only. But if the locations of the lesions were different from those, the results could be also different because the contrast of the masses would change by overlapping with soft tissues. In addition, this study was conducted using the phantom only and did not take into account the effect of heartbeat, which was a very important issue in real examination. We plan to resolve these issues and promote research that is more relevant to actual clinical examination in near future.

4. CONCLUSIONS

We clarified the relationship between the spatial-resolution property in the mass region of DES chest radiograph and the extraction accuracy of the mass region using deep learning. The TTF was used as an index of spatial- resolution property, and the Dice coefficient was also used as an evaluation index for the extracted mass area. They were calculated under different mass occurrence sites and different imaging dose conditions. As a result, the TTFs obtained from the reference dose images and the 75% dose images showed similar frequency characteristics with high Dice coefficients regardless of the locations of the masses. In contrast, when the mass was located in the right supraclavicular region of the 50% dose images, the TTF and the Dice coefficient were obviously lower compared with other conditions. In conclusion, the TTF was strongly related to the extraction accuracy for mass region by deep learning in DES chest radiograph, and 25% dose reduction compared with the conventional dose should be feasible.

REFERENCES

[1] J.E. Kuhlman, J. Collins, G.N. Brooks, et al. Dual-energy subtraction chest radiography: What to Look for Beyond Calcified Nodules. Radiographics, 26(1), 79-92, (2006).

[2] F. Manji, J. Wang, G. Norman, et al. Comparison of dual energy subtraction chest radiography and traditional chest X-rays in the detection of pulmonary nodules. Quant Imaging Med Surg, 6(1), 1-5, (2016).

[3] F. Li, R. Engelmann, K. Doi, et al. Improved detection of small lung cancers with dual-energy subtraction chest radiography. AJR Am J Roentgenol, 190(4), 886-891, (2008).

[4] K. Kishimoto, E. Ariga, R. Ishigaki, et al. Study of appropriate dosing in consideration of image quality and patient dose on the digital radiography. Jpn Soc Radiol Technol, 67(11), 1381-1397, (2011).

[5] K. Honda, Y. Matsui, H. Imai, et al. Regional Distribution of Lung Cancer. Japanese Journal of Lung Cancer, 23(1), 11-21, (1983).

[6] Y. Fujimura, H. Nishiyama, T. Masumoto, et al. Investigation of Reduction of Exposure Dose in Digital Mammography: Relationship between Exposure Dose and Image Processing. Jpn Soc Radiol Technol, 64(2), 259-267 (2008).

[7] O. Rnoneberger, P. Fischer, T. Brox. U-net: Convolutional networks for biomedical image segmentation Lecture Notes in Computer Sciences (including Subser Lect Notes Artif Intell Lect Notes Bioinformatics). 9351, 234-241(2015).

[8] S. Kido, J. Ikezoe, H. Naito, et al. Clinical evaluation of pulmonary nodules with single-exposure dual-energy subtraction chest radiography with an iterative noise reduction algorithm. Radiology, 194(2), 407-412, (1995).

[9] S. Kido, K. Kuriyama, N. Hosomi, et al. Low-cost soft-copy display accuracy in the detection of pulmonary nodules by single-exposure dual energy subtraction: comparison with hard-copy viewing. J Digit Imaging, 13(1), 33-37, (2000)

[10] JR. Wilkie, ML. Giger, MR. Chinander. et al. Investigation of physical image quality indices of a bone densitometry system. Med Phys, 31(4), 873-881, (2004)

[11] S. Kido, H. Nakamura, W. Ito, et al. Computerized detection of pulmonary nodules by single-exposure dual-energy computed radiography of the chest (Part1). Eur J Radiol, 44(3), 198-204, (2002)

[12] S. Kido, K. Kuriyama, C. Kuroda, et al. Detection of simulated pulmonary nodules by single-exposure dual-energy computed radiography of the chest: effect of a computer-aided diagnosis system (Part2). Eur J Radiol, 44(3), 205-209, (2002)

[13] S. Richard, DB. Husarik, G. Yabava. et al. Towards task-based assessment of CT performance: system and object MTF across different reconstruction algorithm. Med Phys, 39(7), 4115-4122, (2012)

[14] B. Sahiner, A. Pezeshk, LM. Hadjiiski. et al. Deep learning in medical imaging and radiation therapy, Med Phys, 46(1), e1-e36, (2018)